Photoemission final states with realistic surface potentials

S. Lorenz[1,3], C.-H. Solterbeck[1], O. Tiedje[1], W. Schattke[1],
J. Burmeister[2] and W. Hackbusch[2]

[1] Institut für Theoretische Physik, Universität Kiel, 24098 Kiel

[2] Mathematisches Seminar - Bereich 2, Universität Kiel, 24098 Kiel,

[3] Fritz-Haber-Institut der Max-Planck-Gesellschaft, 14195 Berlin

Frühjahrstagung der DPG-Münster 1997,
Beitrag O.22.14, Verhandlungen S. 900

Abstract

Scattering states with LEED asymptotics are calculated for general non-muffin tin potentials, as e.g. for a pseudopotential with a suitable barrier and image potential part. The wave function is described with a reciprocal lattice representation parallel to the surface and a discretisation of the real space perpendicular to the surface. The Schrödinger equation leeds then to a system of linear one-dimensional equations. The asymptotic boundary value problem is confined via the quantum transmitting boundary method to a finite interval. The solutions are obtained basing on a multigrid technique which yields a fast and reliable algorithm. The influence of the boundary conditions, the accuracy and the rate of convergence with several multigrid algorithms are discussed. The resulting wave functions and their densities are investigated and applied as final states in photoemission calculations within the one-step model.

MOTIVATION

Photoemission in the ultraviolet frequency spectrum has proved to be an effective tool for the investigation of the surface electronic structure. Because of the finite lifetime of the escaping photoelectron, photoemission is a surface sensitive experiment. Therefore it is important to include a realistic surface potential in the calculations. Structures in the spectra are interpreted as transitions between initial and final states.
The final state of the photoemission is equivalent to the time inverse states of a low energy electron diffraction **(LEED)** system. Being scattering states the final states have to fulfil the LEED-asymptotics of one single incoming plane wave. Many particle effects and inelastic losses are described by a non hermitian optical potential. Thus the wavefunction has to decrease asymptotically in the bulk.
The calculations refer exemplarily to the GaAs (110) - surface. The simplest surface potential model is a step potential. Photoemission spectra basing on matching calculations with such a potential showed the need for an inclusion of a realistic surface potential. The formulation of the problem as a initial value boundary problem in the propagation-matrix method corresponds to an improperly posed problem in the mathematical sense. The results are numerical instabilities in the calculation.

THEORY

It was necessary to re-formulate the problem of finding the solution from the Schrödinger equation with a realistic surface potential of the crystal (see Figures 1 and 2). In the presented method the problem is formulated as a two-side boundary problem. This guarantees the crucial continuous dependence on the boundary conditions. The solution is obtained on a linear grid around the surface. The wave function is described with a reciprocal lattice representation parallel to the surface in the xy plane and a discretisation of the real space perpendicular to the surface in z direction. The basis are plane waves parallel to the surface with coefficients dependent on z. Then the Schrödinger equation leeds to a system of linear one-dimensional equations. This boundary value problem is treated numerically on a finite interval. The presented mixed space calculations are a first step of a full real space calculation for different materials.

CORRUGATED POTENTIAL

The potential barrier takes into account the relaxation of the atoms in the first layers as well as the corrugation. The transition between the crystal and the vacuum is described by a smooth saturated image potential barrier.

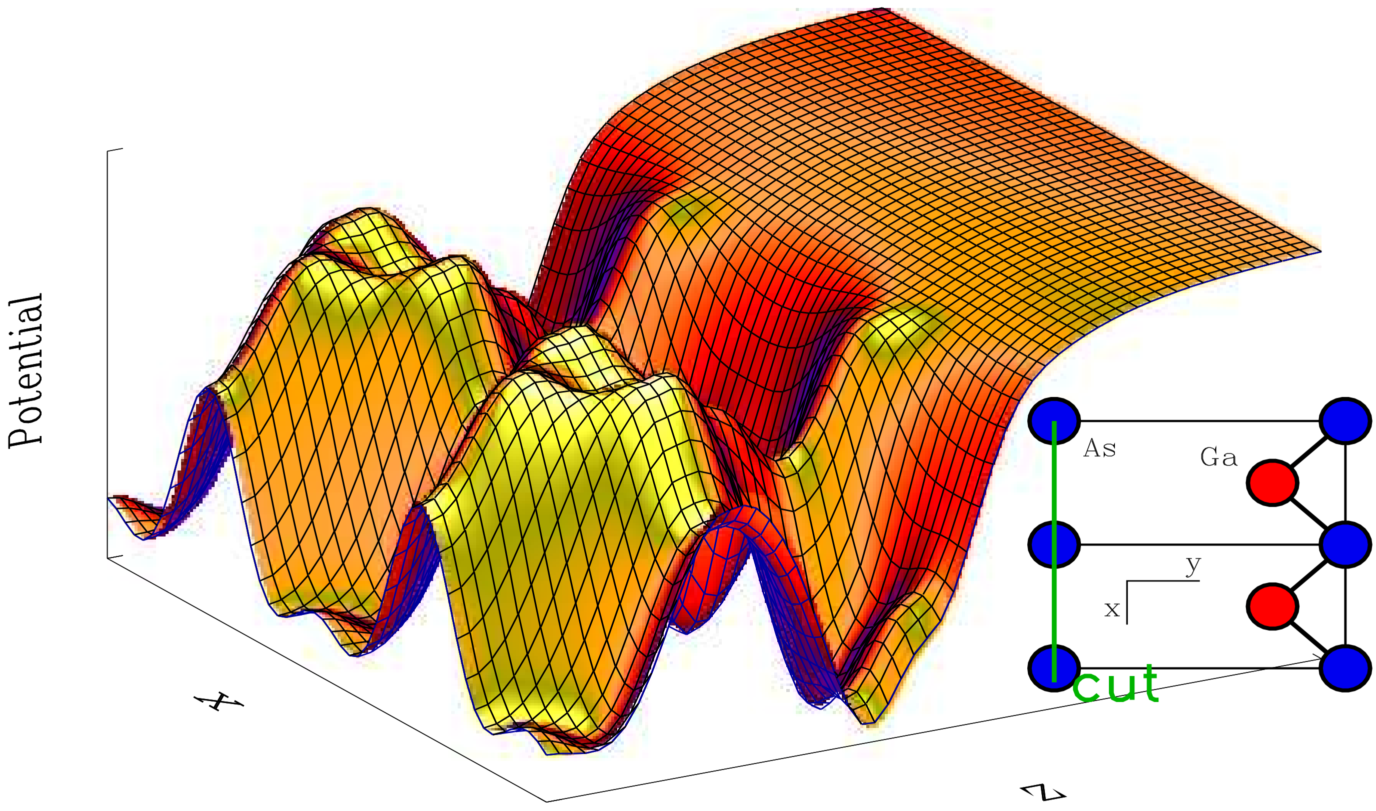

Figure 1: Corrugated potential of the first two layers of the crystal : cut through the arsen atoms.

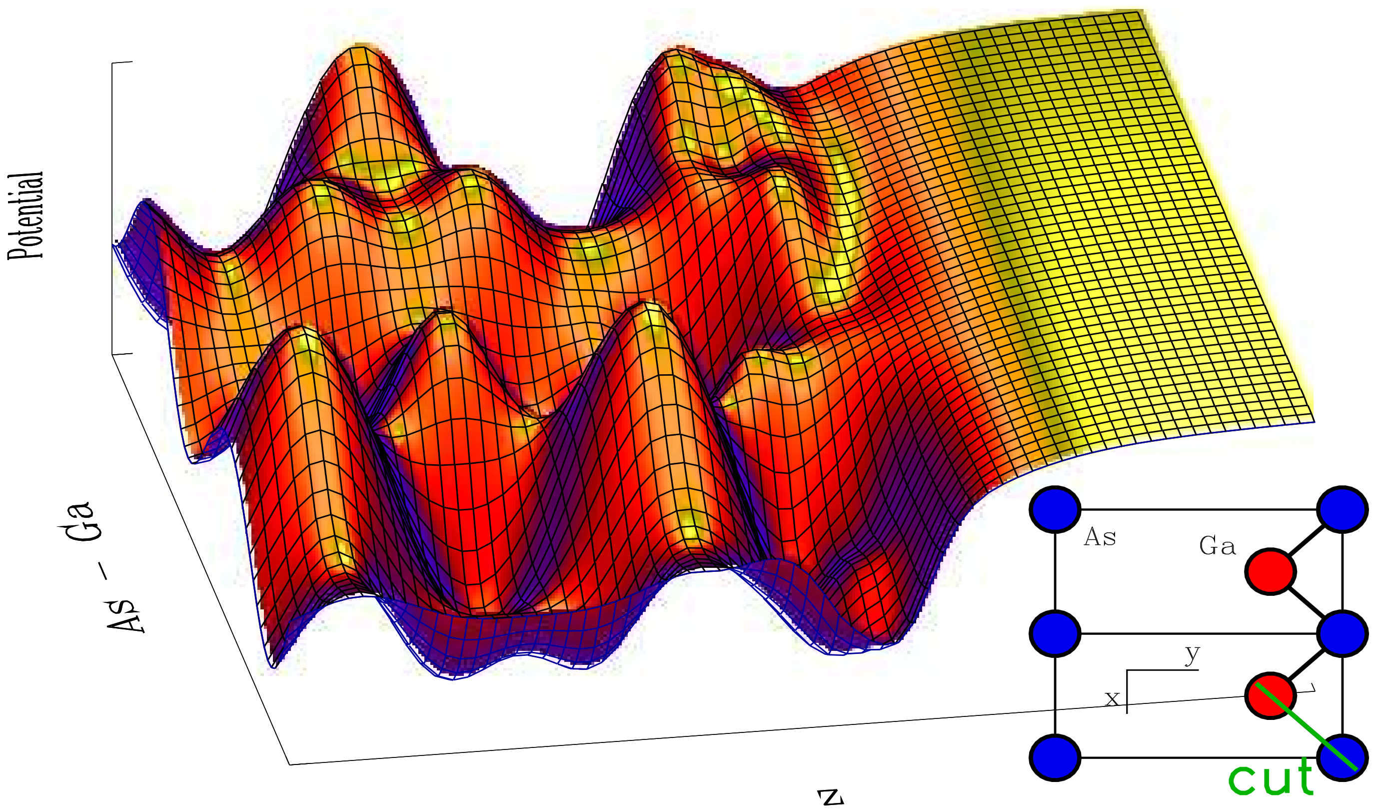

Figure 2: Corrugated potential of the first two layers of the crystal : cut along the binding axis of arsen and gallium.

BOUNDARY CONDITIONS

As a first guess for boundary conditions we take Dirichlet boundaries from a previous *matching* calculation for a step potential.

Bulk Asymptotic

The final state in the bulk has to decrease due to the damping. In Figure 3 the wave functions for different grid sizes are plotted. Plot c) and d) show irregularities around the bulk boundary. Even with Neumann or mixed boundaries this feature cannot be suppressed. If the coordinate of the boundary lies deep in the bulk where the wave function is already zero, the asymptotic is fulfiled. The matching boundary is not any more necessary to be calculated, the value on the boundary can be set to zero. The damping depends on energy. Therefore, the coordinate of the boundary in the bulk may favourably chosen as energy dependent, too.

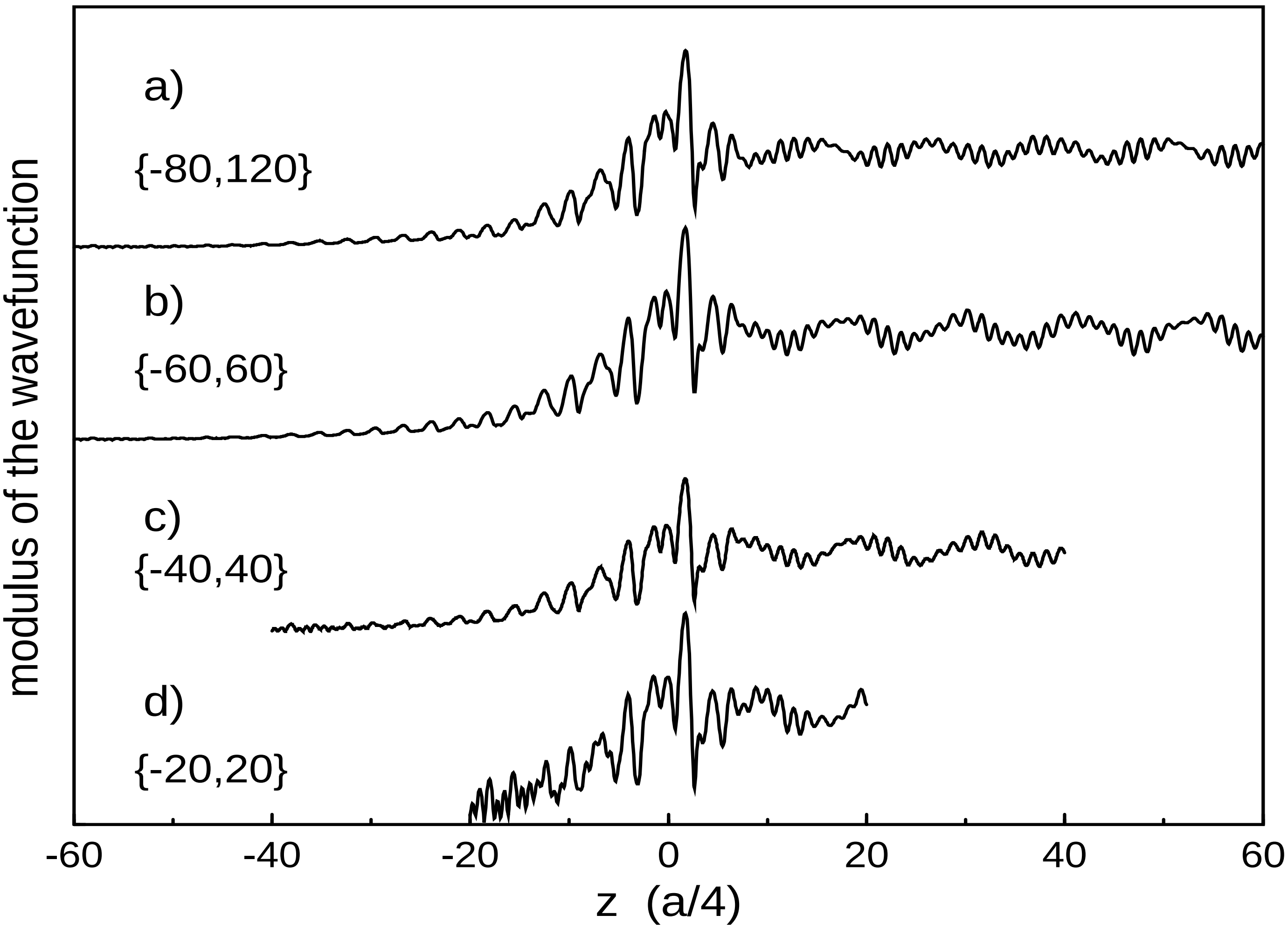

Figure 3: Asymptotics in the bulk: wave functions on different grids. The set of boundaries in $(a/4)$ is printed (lattice constant $a = 5.654\,\mathring{A}$). Mesh size : $h = 0.06\,(a/4)$. Potential : corrugated barrier. $E_f = 18\,eV$.

Vacuum Asymptotic

In a LEED-experiment a beam of electrons is scattered at the surface of the crystal. The vacuum boundary condition has to guarantee one single incoming plane wave. This can be tested by Fourier transforming the vacuum wave function.

• Boundary conditions from matching

For a direct comparison the following grid calculations are also based on a potential step. Figure 4 shows the Fourier spectrum of the matching wave function.

The negative frequencies correspond to the incoming waves. The wave function shows the correct asymptotics with one incoming wave. The Fourier spectrum of the grid wave function in Figure 5 has two additional incoming waves (2 and 3) which do not correspond to the physical situation. Thus, the dirichlet boundaries from the matching are not satisfactory.

Tests with Neumann and mixed boundaries from the matching and an iterative method basing on a Fourier transformation around the vacuum boundary also failed to show the required asymptotics.

Fourier-spectra of the vacuum wave functions with a step potential

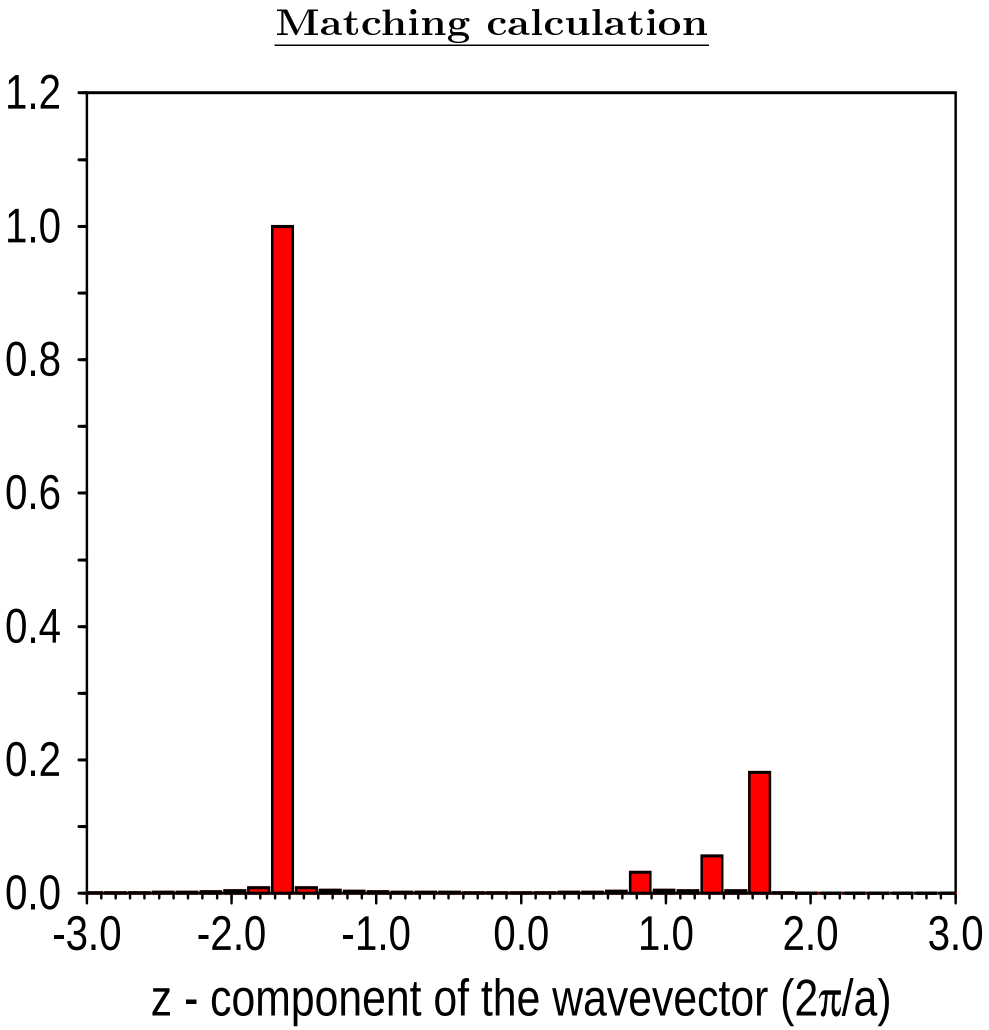

Figure 4: *Matching :* *Fourier-analysis of the vacuum wave function with a step potential.* $E_f = 18\,eV$

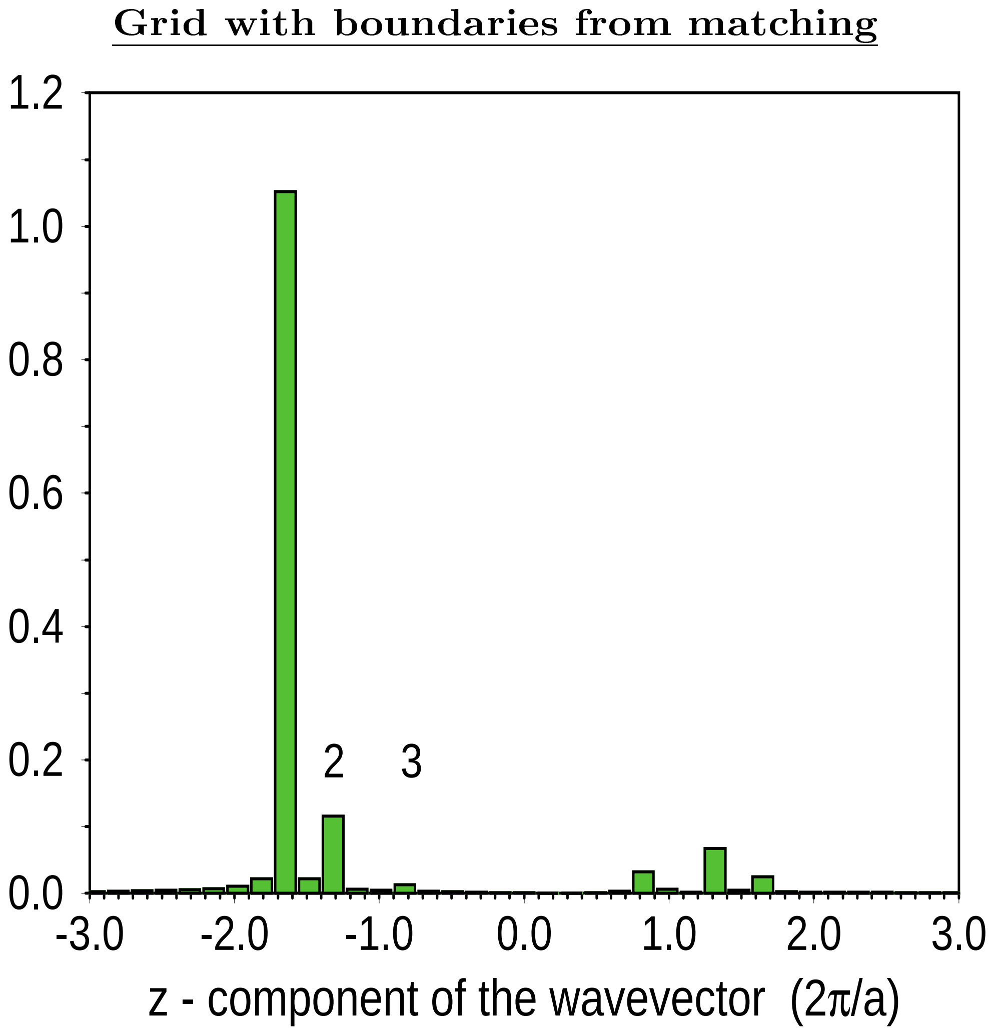

Figure 5: *Grid :* *Fourier-analysis of the vacuum wave function wiht a step potential.* $E_f = 18\,eV$.

• Quantum transmitting boundary conditon

With the *quantum transmitting boundary method (QTBM)* of Lent and Kirkner the asymptotic from the vacuum side is correctly included. This can be seen in Figure 6. The amplitudes of the reflected waves are not equal. This is because the matching wave function intrinsincally contains, even if small, a matching error. However, the essential structures of both wave functions for the step potential in Figure 7 are similar. The QTBM does fulfil the LEED-asymptotics in the case of the corrugated barrier, too.

Comparison between matching and grid with QTBM

Fourier spectra of vaccum wave functions

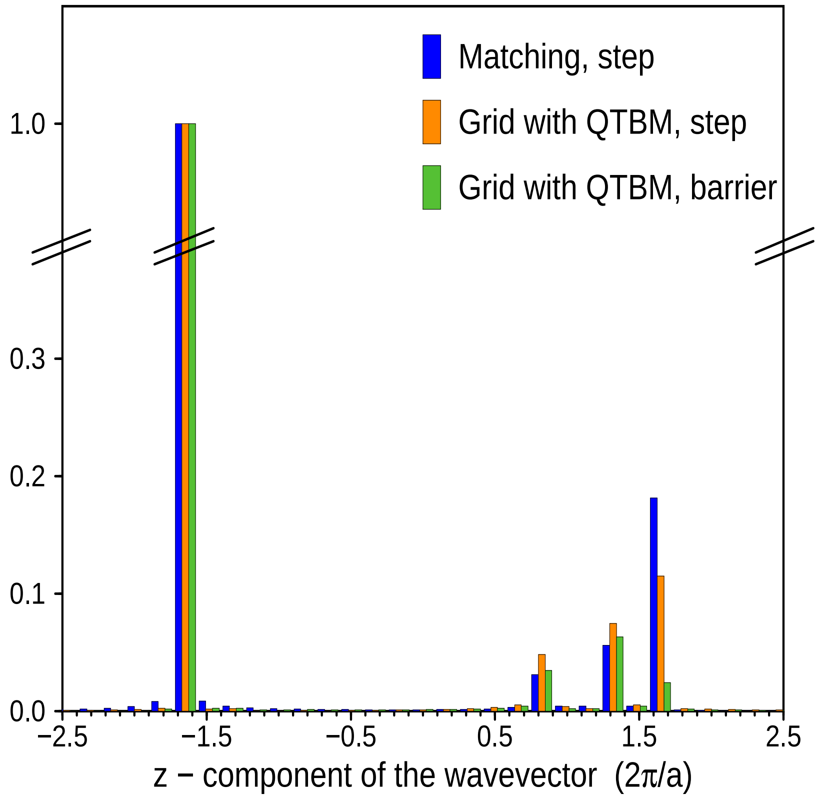

Figure 6: $E_f = 18\,eV$.

Wave functions

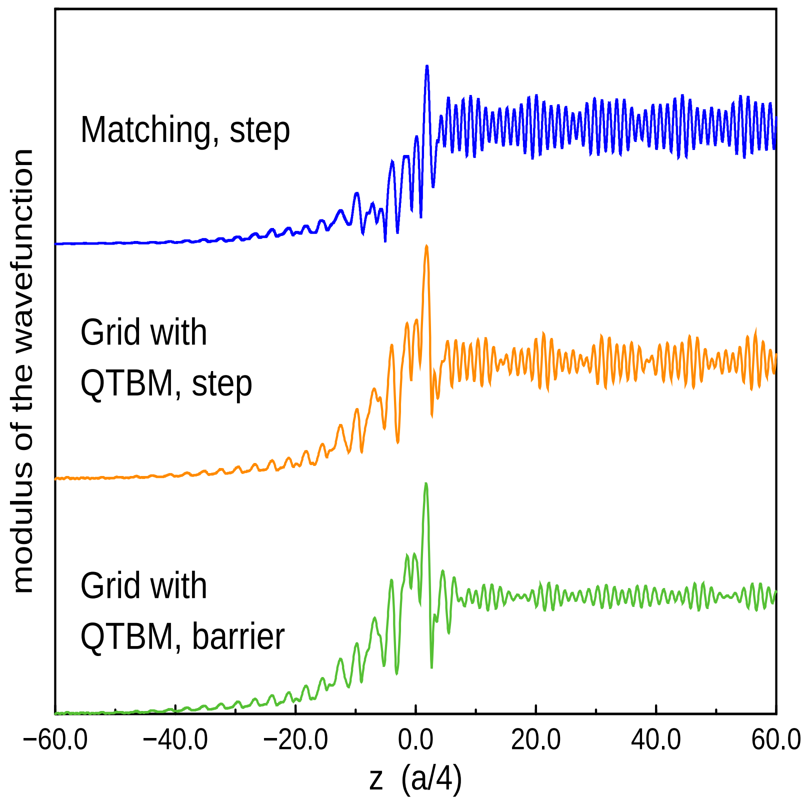

Figure 7: $E_f = 18\,eV$.

CHARACTERISTICS OF THE COEFFICIENT MATRIX

- $(n \cdot M) \times (n \cdot M)$ matrix,
  (n : # surface reciprocal lattice vectors, M : # grid points),
- typical dimension : 142.500 equations ($M = 2500$, $n = 57$),
- non-hermitian due to the damping,
- indefinite and
- block-tridiagonal.

The elements of the coefficient matrix are the potential terms ($\square$), the Laplace term $\triangle = -h_z^{-2}$ and diagonal terms $\mathcal{D}$:

$$
\mathcal{A} = \begin{pmatrix}
\mathcal{D} & \square & \cdots & \square & \triangle & & & & & & & \\
\square & \mathcal{D} & \cdots & \square & & \triangle & & & & & & \\
\vdots & \vdots & \ddots & \vdots & & & \ddots & & & & & \\
\square & \square & \cdots & \mathcal{D} & & & & \triangle & & & & \\
\triangle & & & & \mathcal{D} & \square & \cdots & \square & \triangle & & & \\
& \triangle & & & \square & \mathcal{D} & \cdots & \square & & \triangle & & \\
& & \ddots & & \vdots & \vdots & \ddots & \vdots & & & \ddots & \\
& & & \triangle & \square & \square & \cdots & \mathcal{D} & & & & \triangle \\
& & & & \triangle & & & & \mathcal{D} & \square & \cdots & \square \\
& & & & & \triangle & & & \square & \mathcal{D} & \cdots & \square \\
& & & & & & \ddots & & \vdots & \vdots & \ddots & \vdots \\
& & & & & & & \triangle & \square & \square & \cdots & \mathcal{D}
\end{pmatrix}
$$

DIRECT METHODS

Direct methods are those which give the exact solution of a system of equations within a finite number of operations.

- CPU-time

The CPU-time of different direct solvers in Sparse Matrix Mode and Band Storage Mode was tested on a **CRAY-J916** computer (see Figure 6). In theory the Gaussian elimination for a general matrix needs $O(N^3)$ operations to solve the linear system of equations, when N is the number of unknowns. If the matrix is a band matrix with w codiagonals this can be reduced to $O(N\,w^2)$.

CPU-time

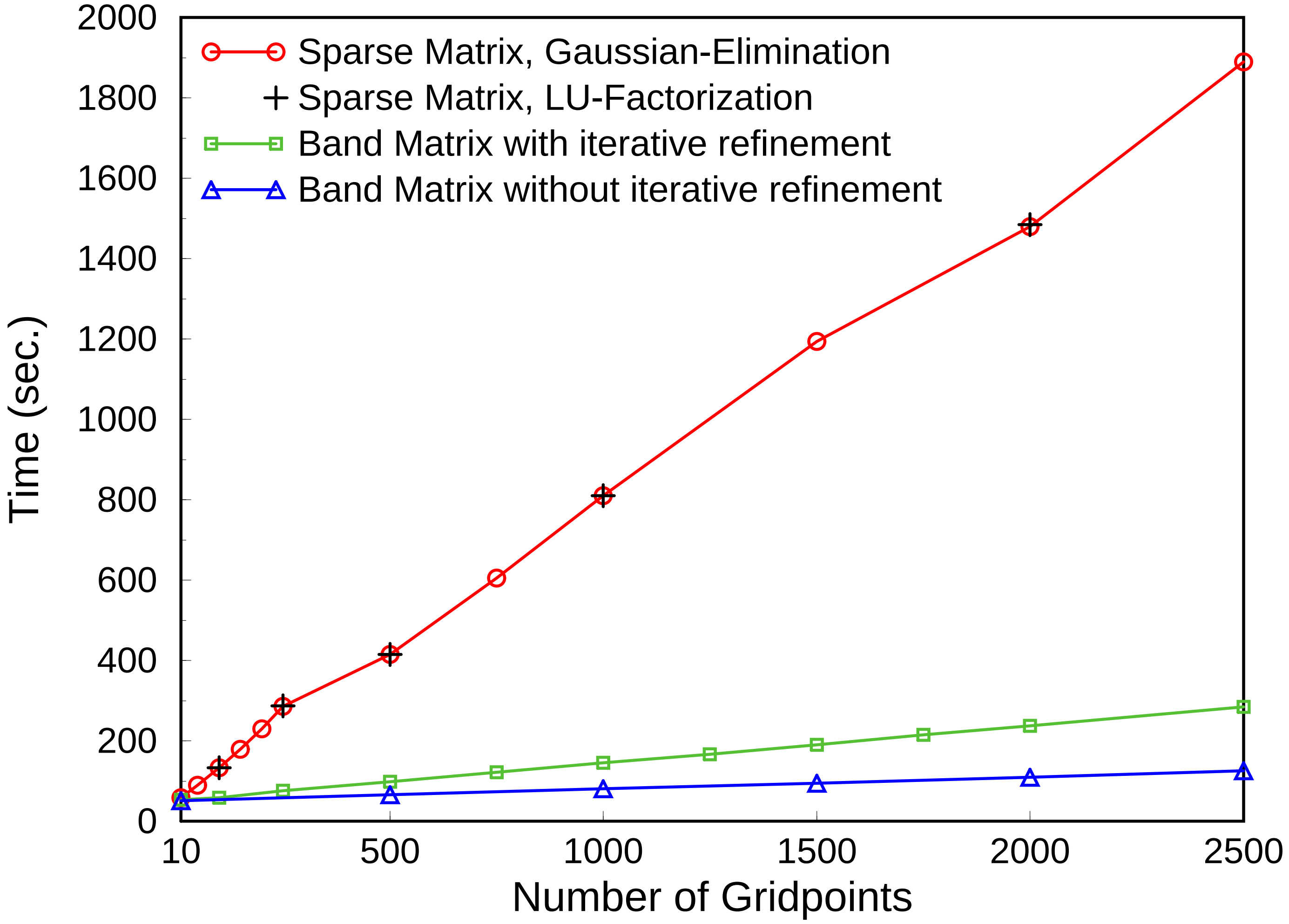

Figure 6: CPU-time.

- Memory

Figure 7 shows the maximum memory used by the different routines. For a general matrix the memory should be equal to N^2+N. For a band matrix one gets $2\,N(w+1)$.

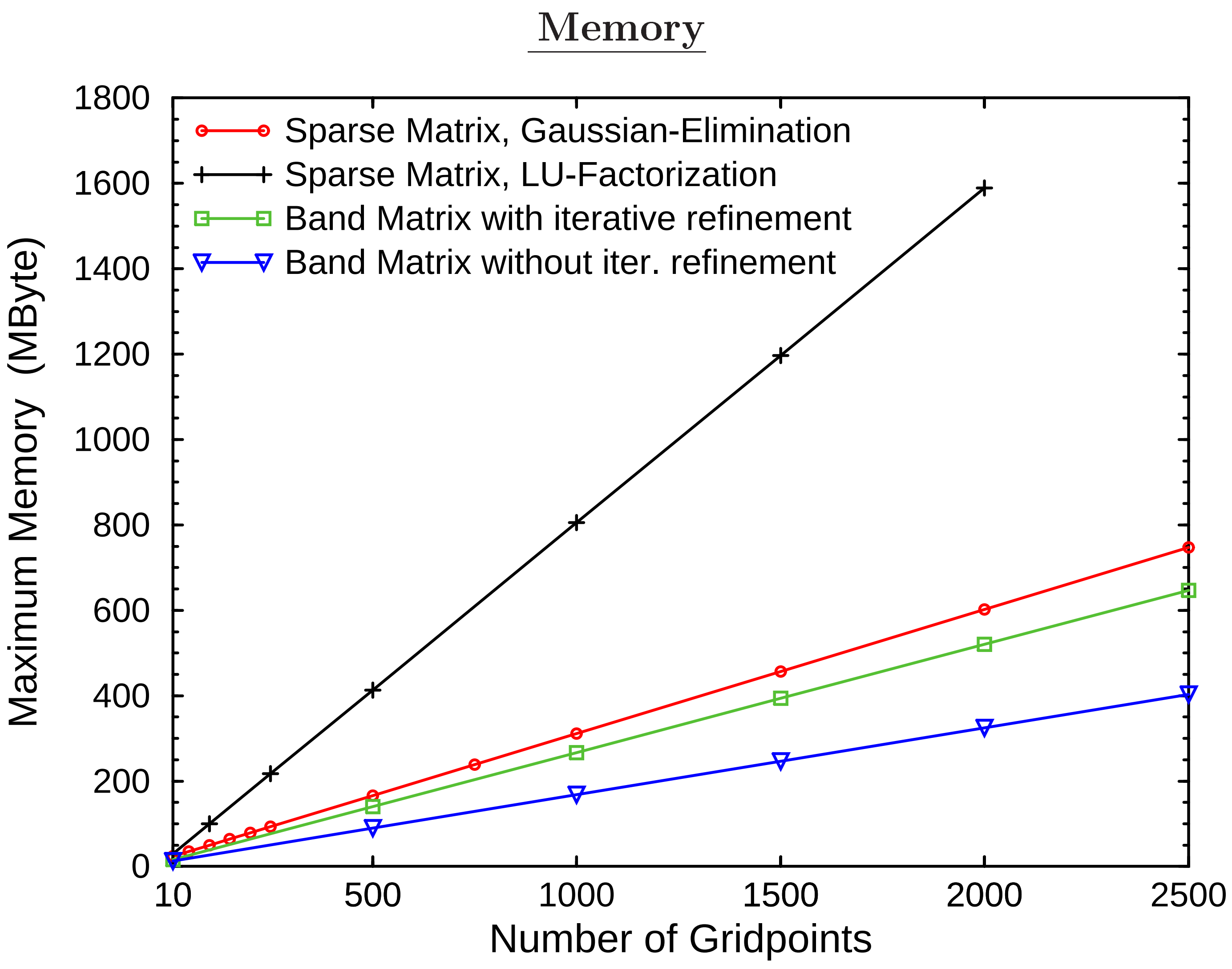

Figure 7: Maximum memory.

MULTIGRID METHODS

We implemented a two- and a three-grid method in a Fortran program. As a smoothing operator the squared Jacobi iteration has been applied. With a damping factor of 0.5 the best convergence rates have been obtained.

- Stability

The mesh size on the coarse grid has to be limited in this type of problem. If the grid on which the solution is directly obtained is not fine enough the multigrid algorithm diverges. This can be understood as follows: The diagonal part of the coefficient matrix can be separated in a Laplace term and a pertubation. If the Laplace term is dominant the multigrid method will **converges** otherwise it **diverges** (see Figure 8).

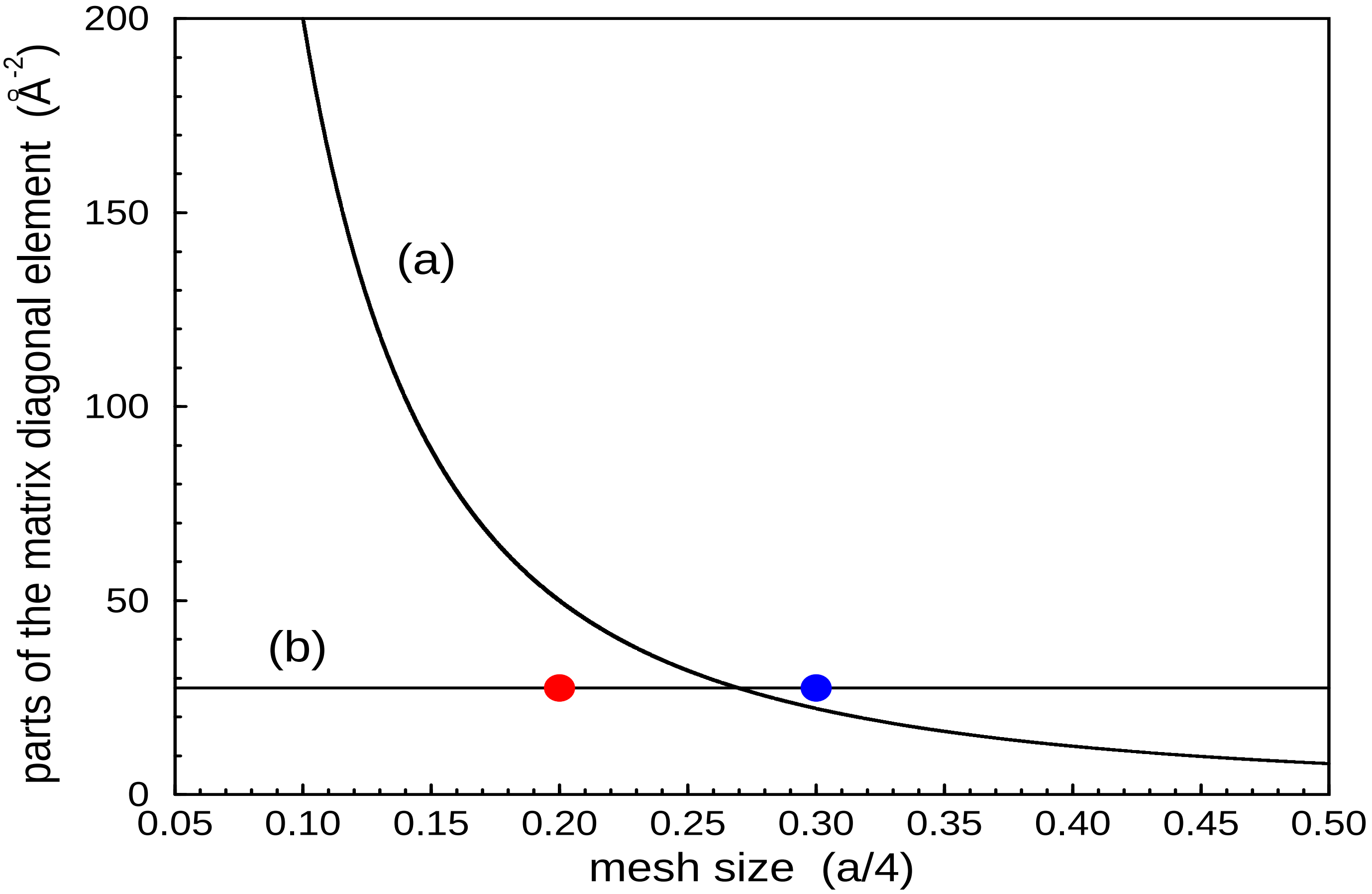

Figure 8: Laplace diagonal part $2h^{-2}$ *(a) against the maximum pertubation at an energy of* $18\,eV$ *(b).*

Convergence **Divergence**

Iteration	$\parallel d_f \parallel$ $h_c = 2h_f = 0.2\,(a/4)$	$\parallel d_f \parallel$ $h_c = 2h_f = 0.3\,(a/4)$
Start	4.7 E-2	4.4 E-2
1	3.5 E-3	4.5 E-3
5	3.4 E-3	8.5 E-2
10	8.3 E-4	1.8
15	2.4 E-4	34.7
20	4.2 E-5	946.1
25	6.8 E-6	21032.2

Table 1: Development of the two-grid defect for two different mesh sizes on the coarse grid.

- **CPU-time**

In theory the multigrid method needs $O(N)$ operations to solve a system of linear equations. The direct method for band matrices needs $O(Nw^2)$ operations. Because the number of codiagonals w is constant both methods have the same asymptotic behaviour. In this special one-dimensional case the multigrid method is not faster than the direct method.
However, if a lower accuracy of the solution is satisfieable the multigrid method becomes competitive. If e.g. a defect of 10^{-6} is sufficient, the two grid method needs 5 Iterations and 91 s and gives an error in the modulus of the wavefunction of less than 0.2 %.

Method	Iterations	$\| d_f \|$	CPU-time (sec.)
direct with refinement		10^{-14}	285
direct without refinement		10^{-14}	98
two-grid	5 / 20	10^{-6} / 10^{-14}	91 / 208
three-grid V-cycle	20	10^{-7}	343
three-grid W-cycle	20	10^{-10}	270

Table 2: CPU-time

• Memory

The maximum memory used can be reduced within the multigrid method. If the system of equations is solved directly only the $(3w+1) \times N$ matrix containing the LU factorization on the "fine" grid is needed. In the multigrid iteration with depth l the $(2w+1) \times N$ matrix on the fine grid and the $(3w+1) \times (N\, 2^{-(l-1)})$ LU matrix on the coarse grid are stored. The development of the amount of memory used in different multigrid levels in comparison to the direct method is presented in Table 3. From the three-grid iteration onwards the memory is reduced.

Direct or Iterative Method	Memory (MByte)
direct (LU + coefficient matrix)	654
direct (only LU)	392
two-grid iteration	458
three-grid iteration	360
four-grid iteration	311

Table 3: Maximum memory used by different solvers (number of grid-points : 2500).

Accuracy of the solution

Figure 9 shows the wave functions of a calculation with the corrugated potential for different mesh sizes. If the mesh size is too big the solution does not correspond to the correct final state. This is due to the sampling theorem. The frequencies in the vaccum part of the wave functions can be calculated from the free electron wave vectors. On a very coarse grid the highest frequencies cannot be represented.

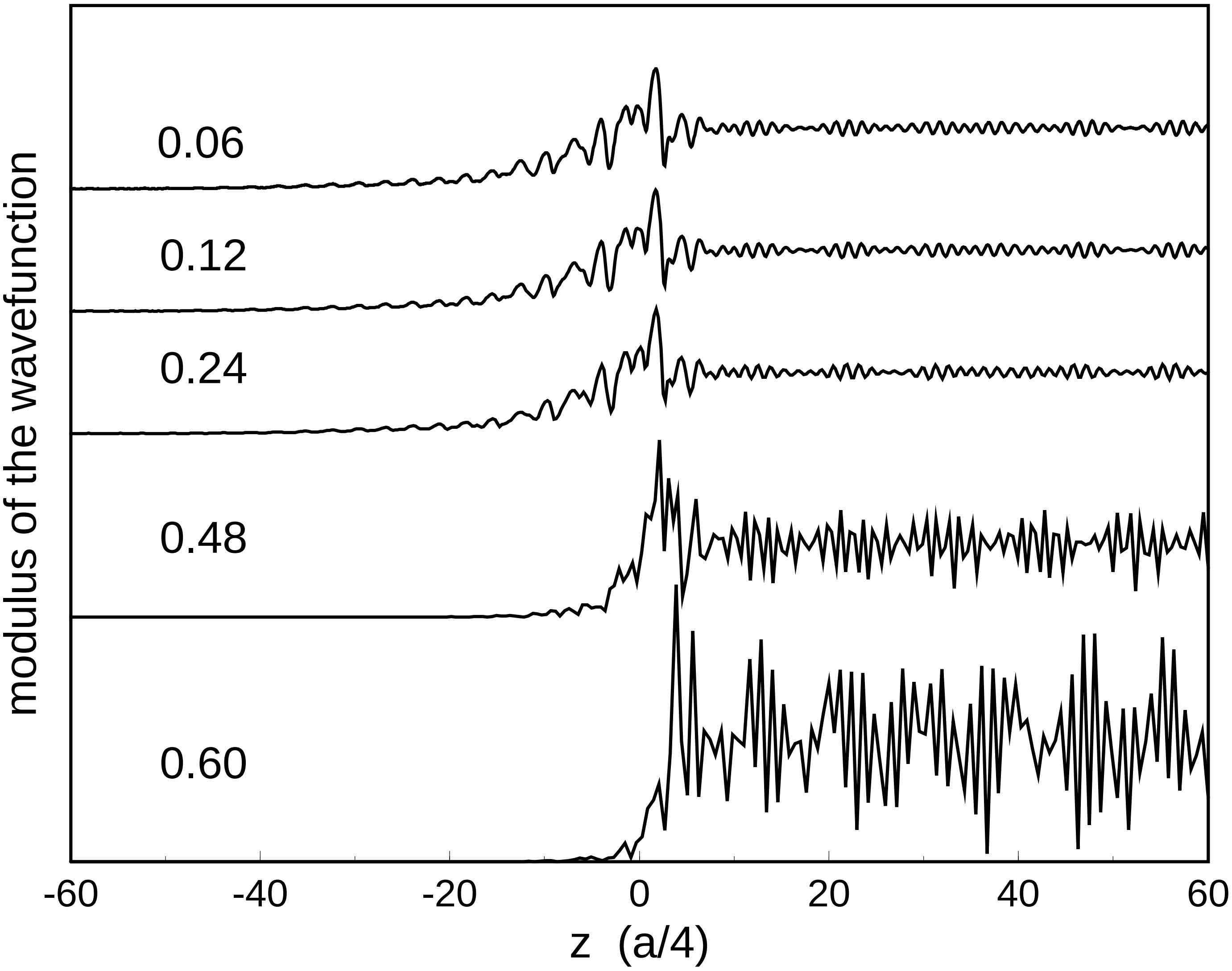

Figure 9: Wavefunctions with corrugated potential and QTBM for different mesh sizes in $(a/4)$. $E_f = 18eV$.

CHARGE DENSITY OF A LEED-STATE

In the representation of the charge density the y- and z-coordinate are varied. The z intervall includes six layers of atoms in the crystal and 1.5 lattice constants into the vaccum. The y intervall covers the length of one unit cell.

The charge density is shown in a surface plot and a contour plot (see Figure 10). The density has its maximum in the planes of the atoms. The interface crystal – vacuum and the exponential decay of the wave function in the crystall are clearly visible.

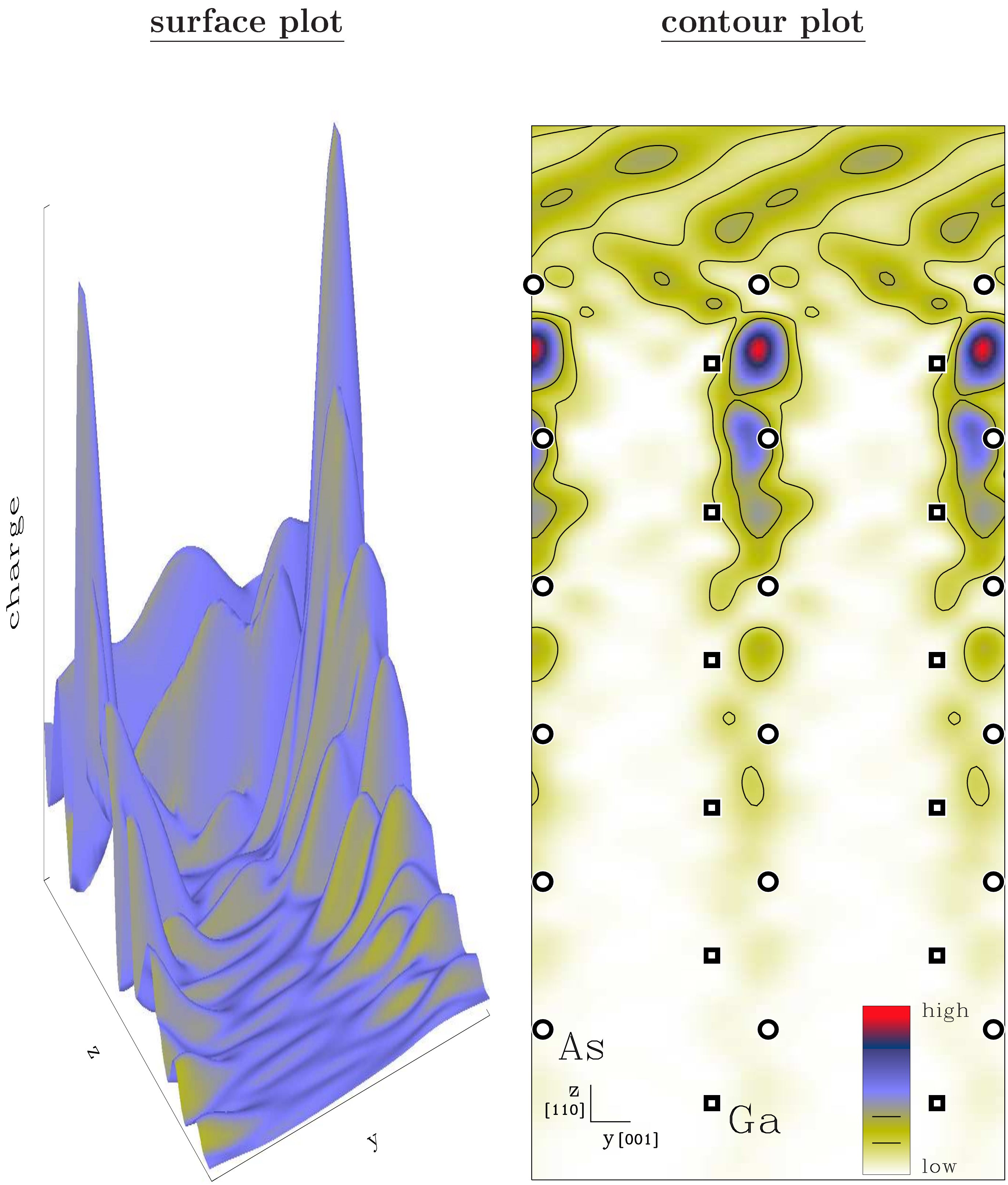

Figure 10: Charge density of a calculation with a corrugated barrier. $E_f = 18eV$.

CONCLUSIONS

- The photoemission final states have been calculated with a realistic potential of the GaAs (110) - surface in real space.

- Different direct solvers of the system of equations have been applied. The fastest was a routine in band storage mode with LU factorization. The time for one final state calculation is nearly 100 CPU-seconds. The CPU-time and the memory show the demanded $O(N)$ - increase.

- A multigrid algorithm with the squared Jacobi method as a smoothing routine has been developed. The coarse grid mesh size was found to be restricted to a limited stepsize. A two-grid iteration took about 200 CPU-seconds. First three-grid calculations were slower.

- The correct LEED-asymptotics were obtained by the quantum transmitting boundary method. The solutions show a distinct dependence on the boundary values with immediate consequences for the photoemission spectra.

- The multigrid method is competitive with direct solvers. An advantage of the multigrid iteration is the possibility of stopping the iteration at a given accuracy. In full real space calculations the method will demonstrate its power.